Strojniški vestnik - Journal of Mechanical Engineering 62(2016)5, 299-306
DOI:10.5545/sv-jme.2015.3200
Original Scientific Paper
Received for review: 2015-11-15
Received revised form: 2016-01-29
Accepted for publication: 2016-03-21

Ductile Behaviour Characterization of Low Carbon Steel: a CDM Approach

K Priya Ajit[1,*] – Abhinav Gautam[2] – Prabir Kumar Sarkar[2]
[1]Indian School of Mines, Department of Mining Machinery Engineering, India
[2]Indian School of Mines, Department of Mechanical Engineering, India

In this paper, the ductile behaviour of two different low carbon steels, C-Mn-440 and interstitial free high strength (IFHS), is presented using a continuum damage mechanics (CDM) approach. The damage growth law is adopted to predict the ductile response of the specified materials. Cyclic load-unload tensile tests in combination with standard uniaxial tensile tests helped to estimate the necessary parameters: damage variable, D, fracture stress, σ_f, threshold damage strain, ε_0, and strain hardening exponent, n, required to apply the model. The strain hardening exponent estimated from the cyclic test data is used to predict the damage variable, D. Increase of damage shows deterioration of the hardening exponent magnitudes varying nonlinearly. The simulated flow curve by the damage variable, D, corresponding to the load-unload test is observed to approximate the experimental true stress-true strain curve very closely up to the onset of necking for both the materials. The experimental values of D, as obtained for C-Mn-440 and IFHS steels, vary from 0.10 to 0.44 and 0.09 to 0.45, respectively. The critical damage parameters, D_C, for the considered materials are 0.44 and 0.45, representing their good ductile response.
Keywords: damage, continuum damage mechanics, modulus degradation, low carbon steel

Highlights
- *The damage parameter is evaluated experimentally through the cyclic load-unload tensile test.*
- *The direct relation between the strain-hardening exponent (n) and damage parameter (D) is revealed.*
- *The damage parameter estimated through chosen model are almost similar to experimental findings.*
- *The flow curve of both the materials coupled with damage shows similar behaviour as the true stress-strain curve before necking.*

0 INTRODUCTION

Ductile damage is a material behaviour demonstrated by diminishing strength with the increasing plastic strain until rupture of the load-bearing member. This is a consequence of micro-separation in metallic polycrystalline aggregates during severe local plastic flow assumed to be caused by a process of evolution of voids or cavities. Voids grow during a high degree of macroscopic plastic flow. These can appear inside the grains, eventually leading to transgranular fracture. The continuum damage mechanics (CDM) encompasses such micro-separations contained in a representative volume element (RVE) viewed at a mesoscale. It defines a damage variable as an effective surface density of void intersections in the RVE plane. A measure of damage helps in formulating its evolutionary laws necessary to depict the ductile response up to fracture for each of the engineering materials [1] and [2]. A constitutive law can then be used to predict the damage governed failure of the structure in service. Its evaluation may provide a guidance requisite to control and secure a better utilization of materials. It can also help post-fracture analysis of components to identify the cause of failure.

Many approaches have emerged to predict damage growth for different kinds of industrial applications since the seminal idea of CDM proposed by Kachanov [3] and Rabotanov [4] for creep in metals. Now damage mechanics is considered to be a viable framework to describe distributed material damage events such as material stiffness degradation, microcrack initiation, growth and coalescence, damage induced anisotropy, etc. Damage mechanics is pervasive in almost every dissipative material degradation process describing creep, fatigue, ductile and brittle damage by their respective model, incorporating the damage-governing parameter [5]. The scope and applications of damage mechanics are now widened to describe all large deformation behaviour for most of the engineering materials.

For nonlinear elastoplasticity coupled with damage as distributed interacting micro-voids, any clear micromechanical model is still a matter of future research. Krajcinovic [6] remarked that a purely micromechanical theory may never replace a properly formulated phenomenological theory as a design tool. The phenomenological CDM-based theories are proposed using the thermodynamics of an irreversible processes, the state variable theory along with physical considerations like the assumption of RVE in the definition of the micromechanical damage variable, the kinetic law of damage growth giving

*Corr. Author's Address: Indian School of Mines, Department of Mining Machinery, Dhanbad, India, ajit160984@gmail.com

strain energy release rate density, plasticity-damage coupling in terms of effective stress, etc.

CDM deals with the phenomena before crack initiation [7]. The CDM law describes the progressive loss of integrity of a material, measurable in terms of a scalar damage variable, D, to predict the ductile behaviour up to fracture. Damage mechanics depicts the microscopic events, such as ductile deformation, fatigue damage, creep, also embrittlement and stress corrosion [8] within its framework. In order to determine the ductile behaviour of a material from CDM, the influence of strain hardening exponent, n, on damage parameter or damage growth has not been explicitly considered thus far. It remains embedded in several damage flow models, however. It is a measure of formability, which is directly related to the ductility and void density. Thus, strain hardening can also be used as a measure of ductile damage. A uniaxial ductile damage model, developed by Bhattacharya and Ellingwood [8], relates damage as a function of plastic strain and strain hardening exponent. In this paper, damage variable estimation from the experimental hardening exponent is shown for the first time.

Low carbon steels, such as IFHS and C-Mn-440, show a good combination of strength and formability. These attributes aid in manufacturing shape-critical structures of automobiles. The current study is accordingly focused on the ductile damage behaviour estimation of these two steels using CDM. The study involves a load-unload cyclic test for direct estimation of the damage variable and other parameters required to show the influence of the strain-hardening exponent on the damage variable, D. The ductile flow behaviour then becomes predictable from the flow model invoking damage D in effective stress term.

1 CONTINUUM DAMAGE MODEL

In the CDM approach, damage is a process involving the growth of micro-voids and micro-cracks expressed by the volume density of micro-cracks and voids in RVE. Damage variable D is assumed to be isotropic, and it physically defines the surface density of one-dimensional micro-cracks and/or micro-separations contained in the plane of RVE. This effect is given by [2]:

$$D = \frac{\partial S_D}{\partial S}, \tag{1}$$

where ∂S_D is the cumulative surface area of micro cracks and ∂S represents the associated area of RVE planes. The critical values of D are D = 0 for undamaged condition and D = 1 for the fully damaged state called "rupture". Now the effective resisting area of undamaged part is assumed to be continuous so that $\partial(\tilde{S}) = \partial S - \partial S_D$. The corresponding effective stress is [2]:

$$\tilde{\sigma}\partial\tilde{S} = \sigma\partial S, \tag{2}$$

$$\tilde{\sigma} = \frac{\sigma\partial S}{\partial\tilde{S}} = \frac{\sigma}{1-D}, \tag{3}$$

here $\tilde{\sigma}$ is the effective stress. The stress in a material's virgin section is replaced by the effective stress term in its damage state. In case of multi-axial isotropic damage, the effective stress tensor is used [2]:

$$\tilde{\sigma}_{ij} = \frac{\sigma_{ij}}{1-D}. \tag{4}$$

Lemaitre [9] states that the strain associated with a stress level on the undamaged body is equivalent to the strain in its damaged state under effective stress. It can be expressed as:

$$\varepsilon = \frac{\sigma}{E} \text{ (undamaged state)}, \tag{5}$$

$$\varepsilon = \frac{\tilde{\sigma}}{E} = \frac{\sigma}{(1-D)E} \text{ (damaged state)}. \tag{6}$$

By using Eqs. (5) and (6), the ductile damage variable becomes:

$$D = 1 - \frac{\tilde{E}}{E}, \tag{7}$$

where $\tilde{E}$ the effective elasticity modulus of damaged material and E is the Young's modulus of virgin material. This relation is one of the best way of expressing ductile damage.

1.1 Thermodynamics of Damage

Evolution of damage is associated with a thermodynamic potential which is the Helmholtz specific free energy ψ. It is assumed here that elasticity and plasticity are uncoupled and provides the law of thermoelasticity coupled with damage [10] and [11]:

$$\psi = \psi_e(\varepsilon_e, T, D) + \psi_P(T, h), \tag{8}$$

where ψ_e is the elastic contribution and function of state variables; ε_e the elastic strain tensor, T the temperature and D the damage variable while ψ_p is the plastic contribution taken to be the function of state variables: temperature T and isotropic hardening h. Treating W_e as the elastic strain energy density (ESED), the elastic energy density release rate (EDRR), Y, becomes:

$$-Y = \frac{W_e}{(1-D)} = \frac{1}{2}\frac{dW_e}{dD}\Big|(\sigma \text{ and } T = \text{constant}). \tag{9}$$

From the concept of strain equivalence and damage equivalent stress, W_e can be expressed in terms of shear energy and hydrostatic energy. Correspondingly, the ESED becomes:

$$W_e = \rho\psi_e^* = \frac{1+\upsilon}{2E}\frac{\sigma_{ij}^D\sigma_{ij}^D}{(1-D)} + \frac{3(1-2\upsilon)}{2E}\frac{\sigma_H\sigma_H}{(1-D)} = \\ = \frac{1+\upsilon}{2E}\left(\frac{2}{3}\right)\frac{\sigma_{eq}^2}{(1-D)} + \frac{3(1-2\upsilon)}{2E}\frac{\sigma_H^2}{(1-D)}. \quad (10)$$

Substituting W_e from Eq. (10) in Eq. (9), the EDRR, Y, becomes:

$$-Y = \frac{\sigma_{eq}^2}{2E(1-D)^2}\left[\frac{2}{3}(1+\nu) + 3(1-2\nu)\left(\frac{\sigma_H}{\sigma_{eq}}\right)^2\right] = \\ = \frac{\tilde{\sigma}_{eq}^{\,2}}{2E}R_v, \quad (11)$$

where σ_H is the hydrostatic stress, $\sigma_{eq} = \sqrt{\left[(3/2)\sigma^D\cdot\sigma^D\right]}$ represents the Mises equivalent stress in which σ^D is the deviatoric stress part of the applied stress state and $\sigma^D\cdot\sigma^D$ is a tensor product. In Eq. (11), σ_H/σ_{eq} is the triaxiality ratio. The ductility measure at fracture decreases as the triaxiality ratio increases [9]. Accordingly R_v is a function of the triaxiality ratio. This is expressed as:

$$R_v = \frac{2}{3}(1-\nu) + 3(1-2\nu)\left(\frac{\sigma_H}{\sigma_{eq}}\right)^2. \quad (12)$$

Most of the CDM models are proposed in terms of dissipation potential and damage variables [10]. The thermodynamic approach ensures that the damage rate $\dot{D}$ be governed by the plastic strain which is introduced through the plastic multiplier ($\dot{\lambda}$) and dissipative damage potential (F_D). According to Lemaitre, the damage rate is given by:

$$\dot{D} = \dot{\lambda}\frac{\partial F_D}{\partial Y}. \quad (13)$$

The plastic multiplier, ($\dot{\lambda}$), represents a scalar multiplier ensuring normal condition of yield function for plastic flow, can be evaluated from the modified constitutive equation of plasticity coupled with damage.

$$\dot{\epsilon_p} = \frac{\dot{\lambda}}{1-D}. \quad (14)$$

Based on the various experimental results, the damage dissipation potential (F_D) is found to be a nonlinear function of EDRR (Y). The expression of F_D is given by:

$$F_D = \frac{S}{(N+1)(1-D)}\left(\frac{Y}{S}\right)^{N+1}, \quad (15)$$

where N is the unified damage law exponent and S signifies energetic damage law parameter. These parameters are a function of temperature and assume a different value for different material.

Substituting $\dot{\epsilon_p}$, the plastic strain rate and F_D, the damage dissipation potential, from Eqs. (14) and (15) into Eq. (13), the unified damage law becomes:

$$\dot{D} = \begin{cases} \left(\frac{Y}{S}\right)\dot{\epsilon_p} & \text{if } \dot{\epsilon_p} \geq \epsilon_0 \\ 0 & \text{if } \dot{\epsilon_p} < \epsilon_0 \end{cases}. \quad (16)$$

The unified damage law under monotonic loading assumes that hardening saturates at σ_u, the ultimate strength. The equivalent stress is then equal to σ_u. Combining Eq. (11) and Eq. (16) also setting R_V=1, the relation for damage rate modifies to:

$$\dot{D} = \left(\frac{\sigma_u^2}{2ES}\right)^N\dot{\epsilon_p}. \quad (17)$$

Then damage parameter D becomes:

$$D = \left(\frac{\sigma_u^2}{2ES}\right)^N(\epsilon_p - \varepsilon_0), \quad (18)$$

where, ϵ_p is plastic strain and ε_0 represents threshold-accumulated plastic strain.

At the seizure of damage evolution, a mesocrack is initiated when the density of defects reaches a value for which the process of localization and instability develops. This represents a material property called "critical damage value", D_C. This is expressed as:

$$D_c = \left(\frac{\sigma_u^2}{2ES}\right)^N(\epsilon_{pR} - \varepsilon_0), \quad (19)$$

where ϵ_{pR} is the local rupture strain in the necking region. Other parameters are as defined above.

1.2 Damage Growth Model for Ductile Material under Uniaxial Loading

In the ductile flow of materials, the strain acts through their difference:

$$\varepsilon_e = \varepsilon - \varepsilon_p, \quad (20)$$

where ε_e is elastic strain, ε_p is plastic strain and ε is the total strain.

A Ramberg-Osgood material obeys the constitutive law:

$$(\sigma / E) = \varepsilon - (\sigma / K)^{1/n}, \quad (21)$$

where, E is the elastic modulus, K is the hardening modulus and n is the strain-hardening exponent.

The free energy per unit volume, ψ, associated with the isotropic damage growth during ductile deformation has its general form presented in [1]:

$$\psi = \int \sigma_{ij} d\varepsilon_{ij} - \gamma(D), \quad (22)$$

where γ is the surface energy of voids and discontinuities that arise due to damage growth, specified per unit volume.

By adding the influence of effective stress and effective strain parts, associated with damage, the elastic and plastic components in Eqs. (20) and (21) are modified. These when used to evaluate the first term of Eq. (22) yeild:

$$\int_0^{\varepsilon} \sigma d\varepsilon = \int_0^{\varepsilon_{e0}} E\varepsilon_e d\varepsilon_e + \int_{\varepsilon_{e0}}^{\varepsilon_e} E(1-D)\varepsilon_e d\varepsilon_e + \int_0^{\varepsilon_p} K{\varepsilon_p}^n d\varepsilon_p + \int_{\varepsilon_0}^{\varepsilon_p} K(1-D)\varepsilon_p^n d\varepsilon_p, \quad (23)$$

where ε_p is plastic strain, ε_0 is threshold strain at the onset of damage growth. The second term, the surface energy density, evaluated from the energy of deforming a plane circle void to a spherical volume, is given as [1]:

$$\gamma = \frac{3}{4}\sigma_f D, \quad (24)$$

where σ_f signifies the true fracture stress. The growth rate of damage with respect to plastic strain is [1]:

$$\frac{dD}{d\varepsilon_p} = -\frac{\sigma_\infty}{\psi_D}\frac{d\varepsilon}{d\varepsilon_p}, \quad (25)$$

where $\psi_D = \partial\psi/\partial D$, is the rate of change of free energy with respect to damage D.

Using the strain equivalence condition of damage the Hollomon plastic flow rule is modified to $\sigma_\infty = K(1-D)\varepsilon_p^n$, where σ_∞ is the remote stress.

By partial differentiation of Eq. (22) with respect to D, gives ψ_D, obtainable as:

$$\psi_D = -\frac{K^2}{2E}\left[\varepsilon_p^{2n} - \varepsilon_0^{2n}\right] - \frac{K}{1+n}\left[\varepsilon_p^{1+n} - \varepsilon_0^{1+n}\right] - \frac{3}{4}\sigma_f. \quad (26)$$

Now, differentiating Eq. (20), with respect to plastic strain, one can find:

$$\frac{d\varepsilon}{d\varepsilon_p} = 1 + \frac{d\varepsilon_e}{d\varepsilon_p}. \quad (27)$$

For the entire practical ductile damage strain range, a near close form solution to Eq. (25) can be obtained by putting $d\varepsilon/d\varepsilon_p$ equivalent to 1 and $K/(2E)$ equivalent to 0. Accordingly, the damage law becomes:

$$D = 1 - \frac{C_2}{\varepsilon_p^{1+n} + C_1}. \quad (28)$$

At the onset of damage evolution, $D=0$ and $\varepsilon_p = \varepsilon_0$. Thus, the constants in Eq. (28) can be estimated from:

$$C_1 = \frac{3}{4}(1+n)\frac{\sigma_f}{K} - \varepsilon_0^{1+n}, \quad (29)$$

$$C_2 = C_1 + \varepsilon_0^{1+n}. \quad (30)$$

For most ductile metals and alloys, the constant C_1 is greater than the plastic strain range of interest. For such a condition, Eq. (28) simplifies to:

$$D = 1 - \frac{C_2}{C_1} + \frac{C_2}{C_1^2}\varepsilon_p^{1+n}. \quad (31)$$

This law, in Eq. (31), specifies damage to be a function of plastic strain and strain hardening exponent.

2 EXPERIMENTAL RESULTS AND DISCUSSION

Among all different possible non-direct methods identified for ductile damage measure of metal under a large amount of deformation, elasticity modulus degradation measure is found to be the most suitable [2]. To evaluate D, a load-unload cyclic tensile test is carried out upto fracture. The effective elastic modulus corresponding to each cycle is captured to estimate D. Other parameters used in the damage law are obtained from load-unload cyclic test as well as uniaxial tensile test for specimens of IFHS and C-Mn-440 steels conforming to ASTM E8 standards [12].

2.1 Uniaxial Tensile Test Evaluation

A uniaxial tensile test is conducted on Instron 8801 keeping strain rate of 10^{-3} s^{-1}. Fig. 1 presents a representative stress-strain diagram for both the materials. Corresponding mechanical properties are presented in Table 1. C-Mn-440 has higher strength, but IFHS steel shows better ductility.

Table 1. Mechanical property of steel

Property	C-Mn-440	IFHS
Yield strength [MPa]	320.97	258.16
Tensile strength [MPa]	452.26	387.59
Elongation [%]	36.55	44.03
Uniform strain [%]	26.2	33.6

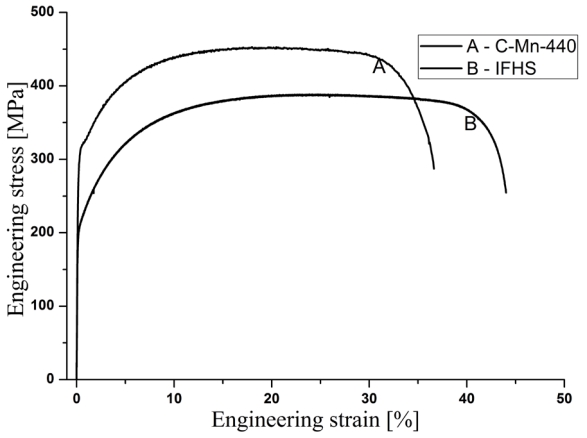

Fig. 1. *Stress-strain curve*

2.2 Load-Unload Tensile Test Evaluation

The damage variable of D is obtained from Eq. (7). Each cycle proceeds with a position controlling of cross-head displacement followed by unloading limit. The tests are performed on Instron 8801 universal testing machine with a strain rate of 10^{-3} s^{-1} in a load-control mode. A set of three specimens are taken for each of the materials. The clip extensometer of 25 mm gauge length gives the strain measure. Fig. 2 provides the resulting stress-strain curve for both the steels. These are used to evaluate D of each cycle. The effective elasticity modulus for each cycle is the slope taken from 15 % to 85 % of the unloading path. This eliminates the effect of nonlinearity at the beginning and the end of the cycle.

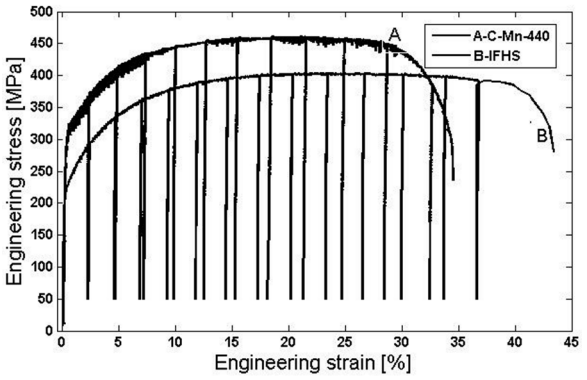

Fig. 2. *A comparative representation of engineering load-unload experimental curves for C-Mn-440 and IFHS Steels*

The effective elastic modulus with increment in plastic strain for each cycle is found to remain almost linear for either of the steels (Fig. 3). The respective values for C-Mn-440 steel varies from 174.65 GPa to 97.63 GPa in the strain range of 2.2 % to 32.4 % and for the IFHS steel, these are from 178.24 GPa to 98.73 GPa in the strain range of 2.2 % to 36 %. The variations in isotropic damage parameter, D, for the chosen steels are shown in Fig. 4. D increases with plastic deformation almost linearly for both the materials. Its magnitudes for C-Mn-440 and IFHS steel are from 0.10 to 0.44 and 0.09 to 0.45, respectively. These are well within the specified range suggested by Lemaitre and Dufailly [2]. At the onset of rupture, D is considered to be critical damage, D_c .Its values for C-Mn-440 and IFHS steels are recorded to be 0.44 and 0.45 respectively. This also conforms to the limits suggested by Lemaitre.

2.3 Effect of Hardening Exponent

From the above-stated test data, variations of strain hardening exponent can be estimated by taking the slope of true stress-strain curve of each step in load-unload cycle test. The Hollomon constitutive relation [13] is used for the purpose:

$$\sigma = K\varepsilon^n. \tag{32}$$

Here, K is the hardening modulus and n designates the strain hardening exponent. The hardening exponent is then obtainable as:

$$n = \frac{d(\log\sigma)}{d(\log\varepsilon)}. \tag{33}$$

The constants in ductile damage model, described in Eq. (31), are now obtainable from the experimental result for both the materials incorporating data from Table 2. A continuous decrement in the hardening exponent is observable up to necking (Fig. 5). This is in agreement with the concept of density deterioration during large tensile elongation. Furthermore, the void density increases with increasing plastic strain [14]. The increase in the void density reduces the effective area available for carrying load, and consequently, the stiffness of the material. With the increase in load, the phenomena of void evolution, growth and coalescence lead to macro-crack formation and growth upto fracture. Thus, a decrease in the hardening exponent increases the rate of damage. The same is observable in the model given by Bhattachrya and Ellingwood (Eq. (31)). These results are shown in Fig. 5 for both of the materials. The damage variable, D, obtained from the test and the model (Eq. (31)) are compared, after incorporating the values of the strain-hardening exponent to indicate the influence of the exponent, in Fig. 6.

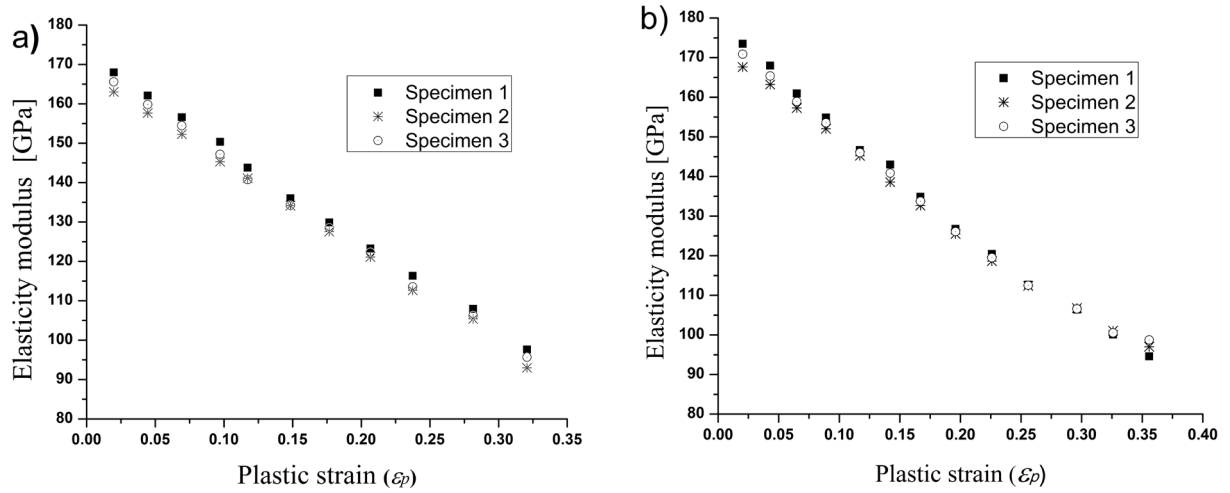

Fig. 3. *Progressive degradation of elastic modulus with strain increment; a) for C-Mn-440 steel, and b) for IFHS steel*

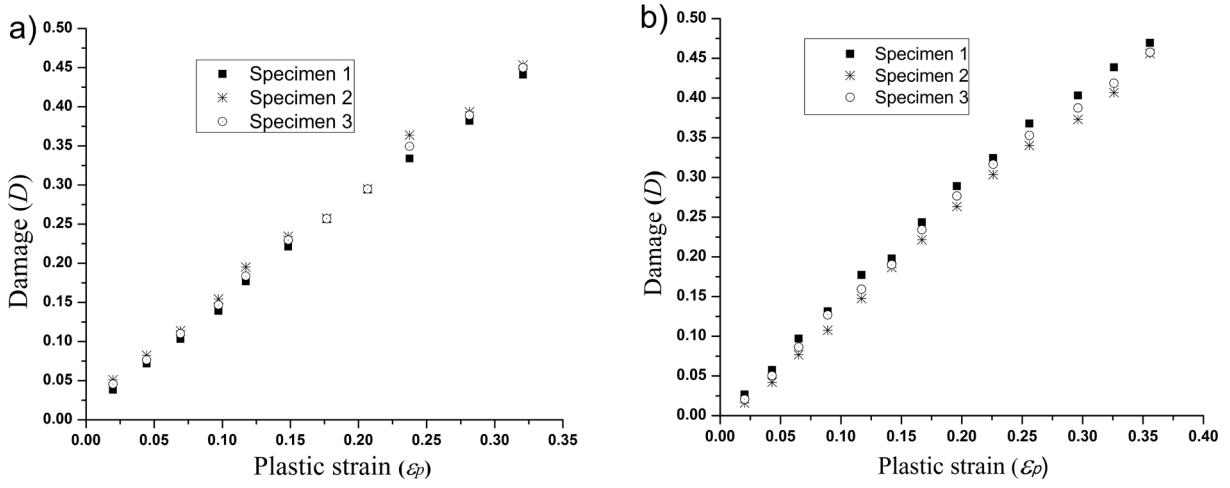

Fig. 4. *Damage evolution with increase in plastic strain; a) for C-Mn-440 steel, and b) for IFHS steel*

Table. 2 *The property values of hardening modulus (K), threshold plastic strain (ε_0) and fracture stress (σ_f) for each of the materials*

Material	True fracture strength (σ_f) [MPa]	Hardening modulus (K) [MPa]	Threshold strain (ε_0)
C-Mn-440	600	732	0.0198
IFHS	515	694	0.020

2.4 Flow Curve Simulation with Damage

The experimental isotropic damage variable is used as the input parameters to recreate the flow characteristic of both the materials. This is designated as the simulated flow curve. These are then compared with the true stress-strain flow curve from the uniaxial tensile test. These are shown in Fig. 7. Good agreement up to the onset of necking is visible. Beyond this point, the curve deviates due to unpredictable change of triaxiality factor. A similar nature of flow curve is observable with AISI1090, AISI1045 and DP590 steels **[15]** and **[16]**.

3 CONCLUSION

An experimental determination of the ductile damage response of C-Mn-440 and IFHS steel is presented. The indirect method of damage evaluation from the load-unload cyclic test is employed to estimate damage variable D and the strain hardening exponent, n. D is shown to be obtainable from the chosen damage growth model (Eq. (31)) by applying strain hardening index, n. The D values for both the materials, obtained from test and by the damage growth law remarkably show identical results. This justifies the fact that strain hardening exponent can also be used as a damage growth measure. The flow curves obtained

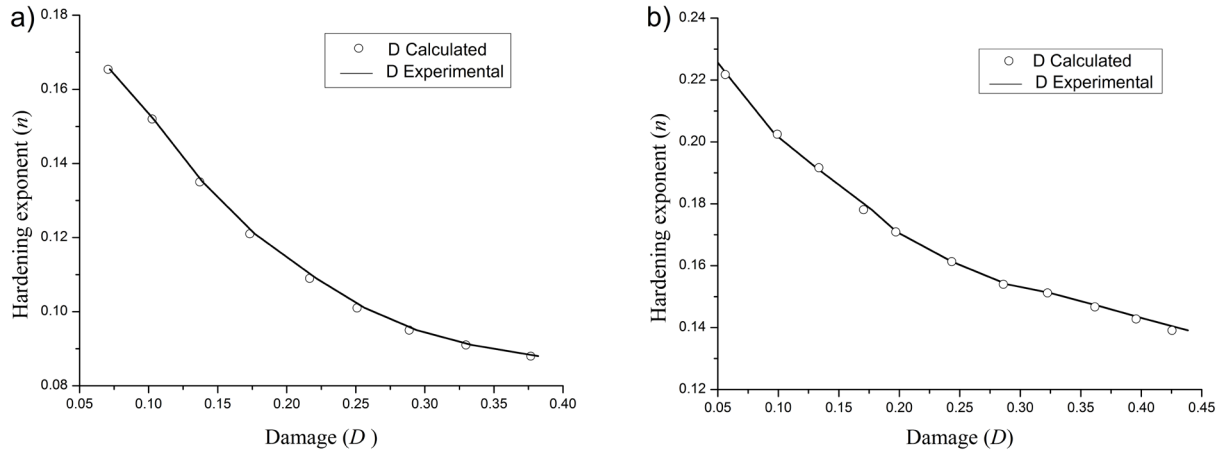

Fig. 5. *Variation of damage with hardening exponent; a) for C-Mn-440, and b) for IFHS*

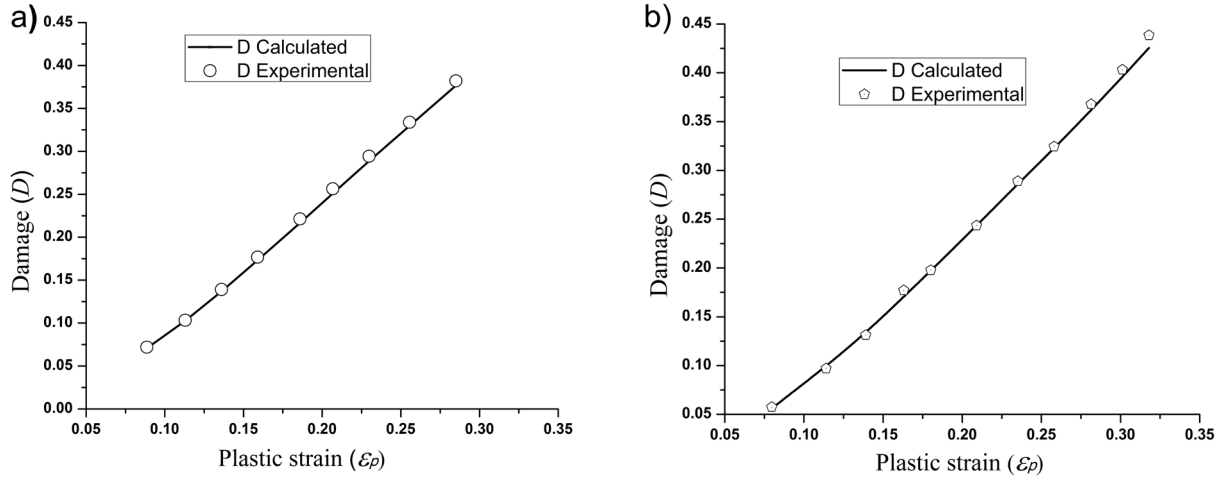

Fig. 6. *A comparison of damage parameter; a) for C-Mn-440, and b) for IFHS*

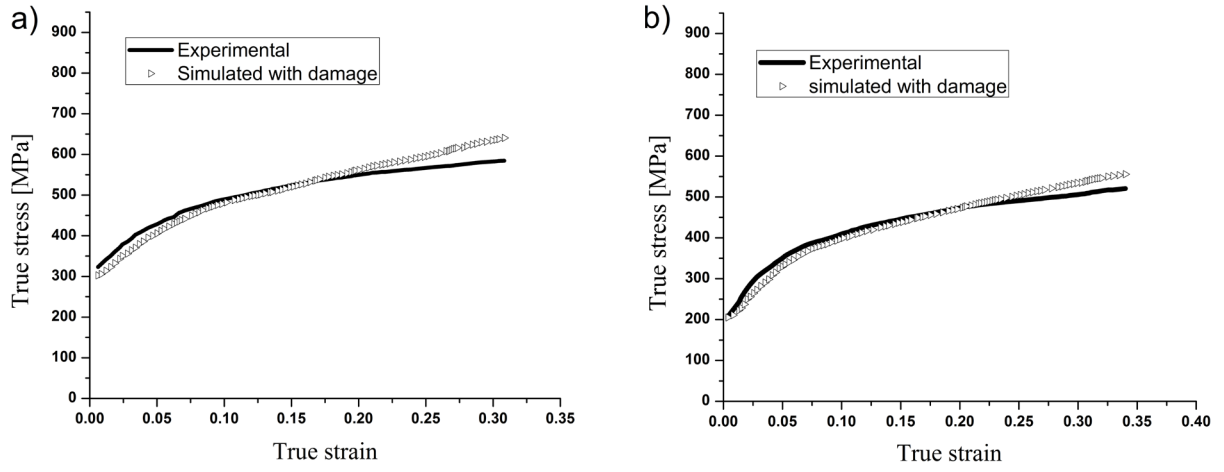

Fig. 7. *A comparison of True stress-strain curve with flow curve coupled with damage; a) for C-Mn-440, and b) for IFHS*

from uniaxial tensile test for both the materials are compared with the simulated CDM-based flow results using the effective stress concept. The flow curves are in close agreement. The chosen model helped to establish that an estimation of strain hardening exponent from load-unload cyclic test is possible, and

it can be used for ductile behaviour estimation. The test data confirms the chosen materials display good ductile in response.

4 REFERENCES

[1] Bhattacharya, B., Ellingwood, B. (1999). A new CDM-based approach to structural deterioration. *International Journal of Solids and Structures*, vol. 36, no. 12, p. 1757-1779, **DOI:10.1016/S0020-7683(98)00057-2**.

[2] Lemaitre, J., Dufailly, J. (1987). Damage measurements. *Engineering Fracture Mechanics*, vol. 28, no. 5-6, p. 643-661, **DOI:10.1016/0013-7944(87)90059-2**.

[3] Kachanov, L.M. (1999). Rupture time under creep conditions. *International Journal of Fracture*, vol. 97, no. 1, p. 11-18, **DOI:10.1023/A:1018671022008**.

[4] Rabotanov, Y.N. (1969). *Creep Problem in Structural Members.* Wiley, Amsterdam.

[5] Lemaitre, J. (1984). How to use damage mechanics. *Nuclear Engineering and Design*, vol. 80, no. 2, p. 233-245, **DOI:10.1016/0029-5493(84)90169-9**.

[6] Krajcinovic, D. (1985). Continuous damage mechanics revisited: Basic concepts and definitions. *Journal of Applied Mechanics*, vol. 52, no. 4, p. 829-834, **DOI:10.1115/1.3169154**.

[7] Chaboche, J.L. (1981). Continuous damage mechanics - A tool to describe phenomena before crack initiation. *Nuclear Engineering and Design*, vol. 64, no. 2, p. 233-247, **DOI:10.1016/0029-5493(81)90007-8**.

[8] Bhattacharya, B., Ellinwood, B. (1998). Continuum damage mechanics analysis of fatigue crack initiation. *International Journal of Fatigue*, vol. 20, no. 9, p. 631-639, **DOI:10.1016/S0142-1123(98)00032-2**.

[9] Lemaitre, J. (1985). A continuous damage mechanics model for ductile fracture. *Journal of Engineering Materials and Technology*, vol. 107, no. 1, p. 83-89. **DOI:10.1115/1.3225775**.

[10] Chaboche, J.L. (1988). Continuum damage mechanics: Part I-General concept. *Journal of Applied Mechanics*, vol. 55, no. 1 p. 59-64, **DOI:10.1115/1.3173661**.

[11] Chaboche, J.L. (1988). Continuum damage mechanics: Part II-damage growth, crack initiation, and crack growth. *Journal of Applied Mechanics*, vol. 55, no. 1, p. 65-72, **DOI:10.1115/1.3173662**.

[12] ASTM E8 / E8M-15a (2015). Standard Test Methods for Tension Testing of Metallic Materials. ASTM International, West Conshohocken, **DOI:10.1520/E0008_E0008M-15A**.

[13] Hollomon, J.H. (1945). Tensile deformation. *Transactions of the Metallurgical Society of AIME*, vol. 162, p. 268-290.

[14] Dieter, G.E. (1928). *Mechanical Metallurgy*, McGraw- Hill book co., Singapore.

[15] Gautam, S.S., Dixit, P.M. (2010). Ductile failure simulation in spherodized steel using a continuum damage mechanics coupled finite element formulation. *International Journal of Computational Methods*, vol. 7, no. 2, p. 319-348, **DOI:10.1142/S0219876210002180**.

[16] Ajit, K.P., Gautam, A., Sarkar, P.K. (2015). Ductile fracture behavior of low carbon high strength steel using continuum damage mechanics. *International Journal of Materials Research*, vol. 106, no. 6, p. 1110-1113, **DOI:10.3139/146.111271**.